Real-time displacement measurement using synchronous detection in a sinusoidal phase modulating interferometer

Takamasa Suzuki
Osami Sasaki
Shuich Takayama
Takeo Maruyama
Niigata University
Faculty of Engineering
8050 Ikarashi 2
Niigata-shi 950-21, Japan

Abstract. A real-time displacement measurement system using a sinusoidal phase modulating interferometer is proposed and demonstrated. The system utilizes the frequency components of the interference signal to detect the desired phase or the displacement in real time. The real-time phase detector is constructed with simple electronic circuits. The system also has a feedback loop to eliminate external disturbance. It is easy to measure the relatively large displacement that exceeds a half wavelength of the light because the compensation circuit is incorporated into the system to obtain continuous phase outside the region from 0 to 2π.

Subject terms: interferometry; laser diodes; synchronous detection; feedback control; phase compensation.

Optical Engineering 32(5), 1033–1037 (May 1993).

1 Introduction

Optical interferometry is an advantageous technique for precise and noncontact measurements. Various kinds of interferometry, such as heterodyne interferometry[1–4] and fringe-scanning interferometry,[5–7] have been proposed. Recently, the laser diode (LD) has been widely used as a light source because of its improved coherence and reliability. Heterodyne interferometers[8] and phase-shifting interferometers[9,10] can be easily constructed using the tunability of the LD wavelength.

Another type of interferometry is sinusoidal phase modulating (SPM) interferometry.[11] The modulation of the LD in an SPM interferometer is very simple compared with that in other interferometers, where the modulating currents must be controlled accurately. In an SPM laser diode interferometer, a sinusoidal modulating current is injected into a constant frequency LD. Feedback control can also be easily introduced to eliminate external disturbances.[12] The phase detection in SPM interferometers is performed with the Fourier transform[13] and integrating-bucket[14,15] methods using a computer.

Recently, real-time measurements became more important because machine control in precise manufacturing requires the detection of microscopic movements. We have proposed methods of real-time precise measurement in SPM interferometry in which synchronous sampling[16] or the phase lock[17,18] is incorporated. The synchronous sampling method uses a peak-hold circuit to obtain a normalized interference signal. When the interference signal amplitude is changed by the external disturbances, the reset control of peak-hold circuit is required. But it is difficult to reset this control exactly. On the other hand, the phase-lock method, which is mainly used for surface profile measurements, requires complex electronic circuits for the feedback control system.

In this paper, we propose another type of real-time displacement measurement. The detection of the SPM interference signal is synchronized with the SPM signal to obtain the first- and second-order harmonics of the SPM frequency. The phase of the interference signal is calculated from these components in digital circuits. The principal of this method, as reported in Ref. 13, uses the fast Fourier transform with a computer. In this interferometer, moreover, the external disturbances that cause variations in the interference signal and decrease measurement accuracy are effectively eliminated by using the feedback control for the LD injection current.

2 Principle of the Real-Time Displacement Measurement

2.1 *Configuration of the Sinusoidal Phase Modulating Interferometer*

Figure 1 shows the setup of the SPM laser diode interferometer for real-time displacement measurement. A Twyman-Green interferometer is used as the optical system. The

Paper 15082 received Aug. 13, 1992; accepted for publication Oct. 3, 1992.

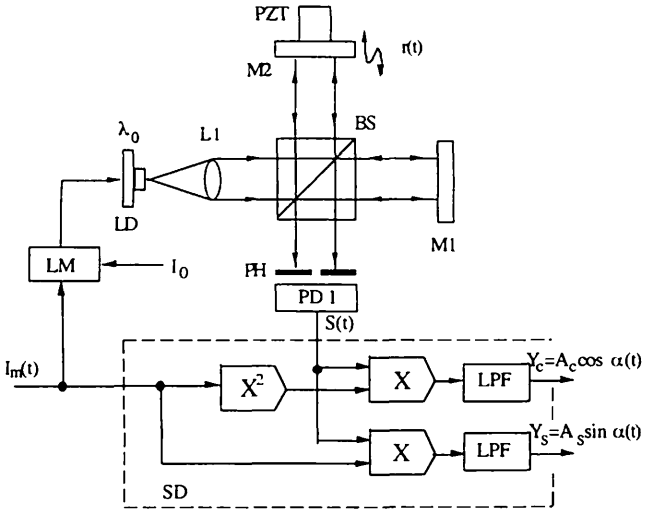

Fig. 1 SPM laser diode interferometer and a synchronous detector.

optical path difference between the two arms is $2D_1$. The injection current of the LD consists of dc bias current I_0 and modulation current $I_m(t)$, which are supplied by the laser diode modulator (LM). Current I_0 determines the central wavelength λ_0 of the LD. The modulation current $I_m(t)$ is

$$I_m(t) = a \cos\omega_c t \ . \tag{1}$$

Because the modulation current changes the wavelength by $\beta I_m(t)$, sinusoidal phase modulation is achieved, where β is the modulation efficiency. The interference signal is detected by photodetector PD1. The time-varying component, or ac component, of interference signal is given by

$$S(t) = S_o \cos[z \cos\omega_c t + \alpha_0 + \alpha(t)] \ , \tag{2}$$

where $z = 4\pi a\beta D_1/\lambda_0^2$, the constant phase α_0 is given by $\alpha_0 = 4\pi D_1/\lambda_0$, and S_0 is the amplitude of the ac component. The phase $\alpha(t)$ is given by

$$\alpha(t) = 4\pi r(t)/\lambda_0 \ , \tag{3}$$

where $r(t)$ is the displacement of an object.

2.2 *Principle of Synchronous Detection*

The interference signal $S(t)$ and the modulation current $I_m(t)$ are led to the synchronous detector (SD) to obtain the orthogonal components, or $\sin\alpha(t)$ and $\cos\alpha(t)$. The block diagram of the SD is shown in Fig. 1. Expanding Eq. (2) by ignoring the constant phase α_0, we obtain

$$S(t) = S_0 \cos\alpha(t)[J_0(z) - 2J_2(z)\cos 2\omega_c t + \cdots] - S_0 \sin\alpha(t)[2J_1(z)\cos\omega_c t - 2J_3(z)\cos 3\omega_c t + \cdots] \ , \tag{4}$$

where $J_n(z)$ is an n'th-order Bessel function. Multiplying $S(t)$ by $I_m(t)$ and passing it through the low-pass filter (LPF), we obtain the signal associated with the frequency component of ω_c as follows:

$$Y_s = A_s \sin\alpha(t) \ , \tag{5}$$

where $A_s = -2K_1 S_0 a J_1(z)$ and K_1 is the LPF1 gain. Squaring $I_m(t)$ and suppressing the dc component of $I_m^2(t)$, we obtain the signal

$$I_{m2}(t) = (a^2/2)\cos 2\omega_c t \ . \tag{6}$$

By using $I_{m2}(t)$, the following signal associated with the frequency component of $2\omega_c$ is obtained in the same manner as Eq. (5):

$$Y_c = A_c \cos\alpha(t) \ , \tag{7}$$

where $A_c = -K_2 S_0 a^2 J_2(z)$ and K_2 is the LPF2 gain. The signal processing to obtain the signal of Eqs. (5) and (7) are the so-called synchronous detections. When K_1 and K_2 are set so that $A = A_s = A_c$, the phase $\alpha(t)$ is calculated from

$$\alpha(t) = \tan^{-1}(Y_s/Y_c) \ . \tag{8}$$

2.3 *Principle of Real-Time Phase Detection*

To obtain $\alpha(t)$ in real time we use the digital circuit and the arctangent conversion table instead of a computer. The block diagram of the phase detector is shown in Fig.2. The signals Y_s and Y_c are converted to 8-bit digital values by 8-bit analog-to-digital (A/D) converters. The sampling clock for the A/D converters is generated from the modulation current $I_m(t)$ using the zero-cross circuit, so the sampling frequency is equal to the modulation frequency $\omega_c/2\pi$. The outputs of the A/D converters, say digitized Y_s and Y_c, are used as the row and column addresses, respectively, of the 8-bit read-only memory (ROM). The contents of the ROM are shown in Fig. 3. The desired α's have been calculated in advance using Eq. (8) for all the combinations of Y_s and Y_c and written in the ROM. The data 0 and 255 in the ROM are equivalent to 0 rad and 2π rad, respectively, so the phase resolution is $2\pi/255$ rad. Because α is defined in the region of 0 to 2π, the detected phase should be compensated to be continuous when the change in α exceeds 2π. This process is carried out with the compensation circuit (CC). The procedure for the compensation is shown in Table 1. The detected phase α becomes discontinuous at $\alpha = 0$ or in the region of $Y_c > 0$, as shown in Fig. 3. In that region, if the sign of Y_s changes from minus to plus, we judge that the phase increases and add 2π to α. Inversely, if the sign of Y_s changes from plus to minus, we judge that the phase decreases and subtract 2π from α. The block diagram of the CC is shown in Fig. 4. It is constructed with flip-flops (FFs) and a 4-bit binary up-down counter, which is gated by Y_c. The FFs latch the sign of Y_s synchronously with the sampling clock. The signs of Y_s and Y_c are judged by their most significant bit (MSB), and FF1 and FF2 detect the positive and negative edge, respectively. The outputs of the FFs are led to the up-down counter only when the sign of Y_c is plus. Consequently the CC acts according to the procedure shown in Table 1, and the 4-bit digital value is obtained for compensation when the phase changes outside the region of 0 to 2π. The 8-bit data from the ROM and the 4-bit data from the CC are fed to a 12-bit digital-to-analog (D/A) converter and the phase change can be observed in real time. The 12-bit data represents the phase 0 to $2\pi \times 2^4$.

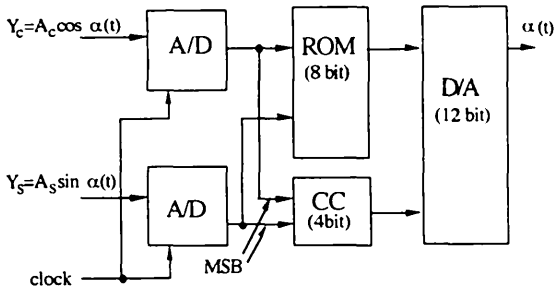

Fig. 2 Block diagram of real-time phase detector.

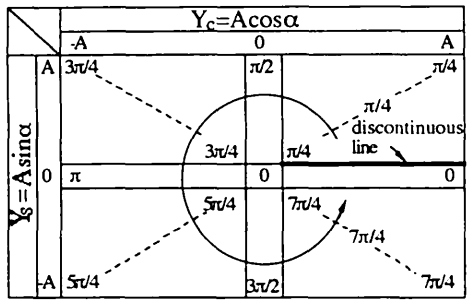

Fig. 3 Contents of the ROM.

Table 1 Procedure for the phase compensation.

Sign of cosα	Change of sign of sin α	Compensative value
+	- +	+2π
	+ -	-2π

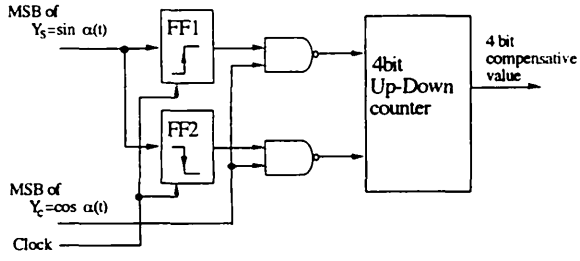

Fig. 4 Block diagram of the phase compensation circuit.

3 Influence of the LPF in Synchronous Detection

Although the maximum value of the measurable phase change is expanded to $2\pi \times 2^4$ using the CC, it is limited by the cutoff frequency of the LPF used in the synchronous detection. To consider this limitation, we suppose that the displacement $r(t)$ is

$$r(t) = d \sin\omega_r t \ . \tag{9}$$

From Eqs. (3) and (5), the signal Y_s becomes

$$Y_s = A \sin(z_r \sin\omega_r t) \ , \tag{10}$$

where $z_r = 4\pi d/\lambda_0$. The expansion of Eq. (10) is given by

$$Y_s = A[2J_1(z_r) \sin\omega_r t + 2J_3(z_r) \sin\omega_r t + \cdots] \ , \tag{11}$$

where Y_s contains the high-frequency component whose amplitude depends on z_r. Similarly, Y_c is represented by

$$Y_c = A[J_0(z_r) + 2J_2(z_r) \cos 2\omega_r t + 2J_4(z_r) \cos 4\omega_r t + \cdots] \ . \tag{12}$$

Because the synchronous detection uses an LPF whose cutoff frequency is ω_f, the frequency components that are higher than ω_f are eliminated from Y_s and Y_c. So the signals Y_s and Y_c become distorted, Y_s' and Y_c'. Then, the detected vibration $r'(t)$ is given by

$$r'(t) = (\lambda_0/4\pi) \tan^{-1}(Y_s'/Y_c') \ . \tag{13}$$

We estimated the measurement accuracy using the root-mean-square (rms) error calculated from the difference between Eqs. (9) and (13) over one period of the vibration. The calculation results are shown in Fig. 5. Although the rms error is considerably affected by the eliminated frequency components, it converges to zero rapidly as the frequency ratio ω_r/ω_f becomes small. For example, when $\omega_r/\omega_f = 10^{-1}$, we can accurately measure the vibrations up to $d = 400$ nm. Consequently, the cutoff frequency ω_f must be selected by considering the frequency bandwidths of Y_s and Y_c.

4 Experiments

The experimental setup is shown in Fig. 6. The system contains two Twyman-Green interferometers; one (SYS1) is used for the displacement measurement system and the other (SYS2) is used for the feedback control to eliminate the external disturbance. The optical path differences between the two arms are $2D_1$ and $2D_2$, respectively, and they are set to $2D_1 = 2D_2 = 100$ mm. A beamsplitter (BS1) separates the two interferometers. A GaAlAs laser diode (HITACHI HL7801E) is used. Its maximum output power is 5 mW and the central wavelength λ_0 is 780 nm. The modulation efficiency β of the LD is 6.0×10^{-3} nm/mA. The frequency of phase modulation $\omega_c/2\pi$ was set to 10 kHz. The cutoff frequency $\omega_f/2\pi$ of the LPF was set to one tenth of modulation frequency to eliminate the carrier components sufficiently.

The external disturbance $d_2(t)$ is detected as a phase change in the interference signal $S_2(t)$ in SYS2. The feedback signal $Y_f(t) = A_f \sin\delta_2(t)$ is produced in a feedback signal generator (FBSG) by the synchronous detection procedure. The $Y_f(t)$ is fed to the amplifier, whose gain is K_p, and the control current $I_c(t)$ is produced. Consequently, the phase change introduced by the external disturbance is compensated by the change in wavelength $\beta I_c(t)$. The principle and the effect of the feedback control are shown in Ref. 12 and are not explained in detail here.

Now we show some experimental results using the setup shown in Fig. 6. The object is mirror M2 mounted on a piezoelectric transducer (PZT).

First, mirror M2 was driven by the PZT sinusoidally. Its amplitude and frequency were 400 nm and 100 Hz, respectively. The amplitude of the vibration has been calibrated by another method, which is described in Ref. 12.

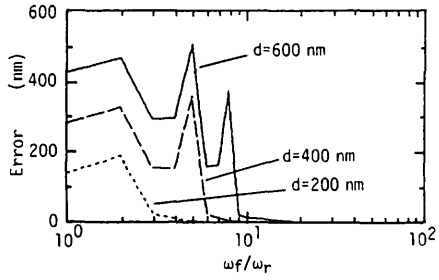

Fig. 5 The rms error calculated from the difference between original sinusoidal vibration $r(t)$ and detected vibration $r'(t)$. The horizontal axis shows the ratio between the vibrating frequency and the cutoff frequency of the LPF.

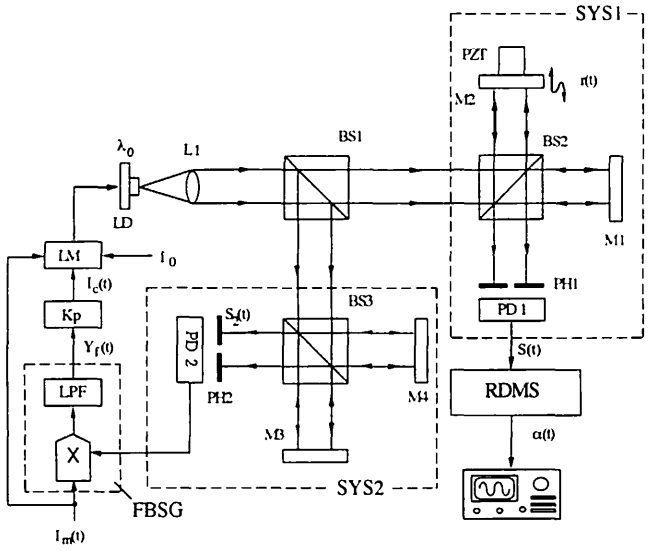

Fig. 6 Experimental setup of the real-time displacement measurement system with feedback control.

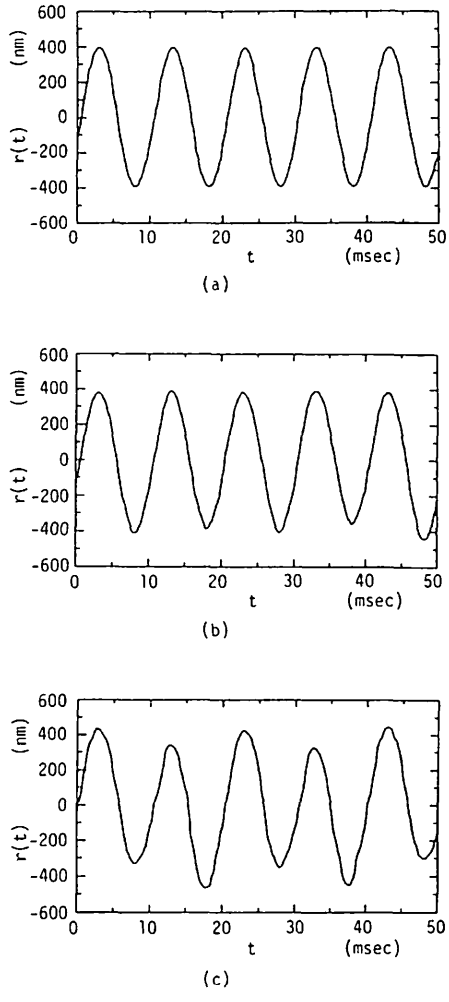

Fig. 7 (a) Sinusoidal vibration applied to PZT, measured vibrations with our system (b) when the feedback control is used and (c) when the feedback control is not used.

The results of the measurement are shown in Fig. 7. Figure 7(a) shows the driving signal for the PZT. The vertical axis is converted from applied voltage to displacement. The results of measurement when feedback control, or SYS2, was used are shown in Fig. 7(b). Figures 7(a) and 7(b) agree well, which shows that a large displacement, more than $\lambda/2$, can be measured with high accuracy in our system. On the other hand, when the feedback control was not used, the displacement detected was as shown in Fig. 7(c), where the sinusoidal form can be observed, but the external disturbance is superimposed with a low frequency on the desired signal. A comparison of Figs. 7(b) and 7(c) shows the effect of feedback control.

Next, we measured the triangular vibration whose amplitude and frequency were 400 nm and 100 Hz, respectively, using the feedback control. The results are shown in Fig. 8. The external disturbances are almost eliminated and the triangle vibration is detected accurately.

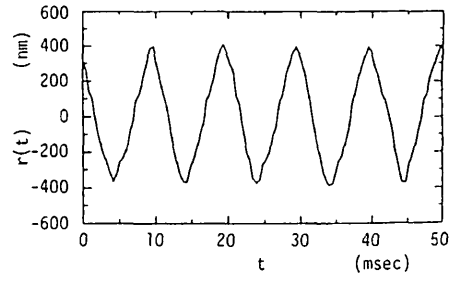

Fig. 8 Triangle vibration measured using the feedback control.

5 Conclusions

We proposed and demonstrated a real-time displacement measurement system that uses a simple circuit. Although the measurable range and frequency in the sinusoidal signal mainly depend on the cutoff frequency of the low-pass filter in the synchronous detector, it is easy to measure a large vibration, exceeding $\lambda/2$, at the appropriate cutoff frequency. Highly accurate measurement, free from external disturbance, can be carried out using the feedback control in this system. It is useful for the relatively large displacement measurement.

References

1. K. D. Stumpf, "Real-time interferometer," *Opt. Eng.* **18**, 648–653 (1979).
2. N. A. Massie, "Real-time digital heterodyne interferometry: a system," *Appl. Opt.* **19**, 154–160 (1980).
3. G. E. Sommargren, "Optical heterodyne profilometry," *Appl. Opt.* **20**, 610–618 (1981).
4. D. Pantzer, J. Politch, and L. Ek, "Heterodyne profiling instrument for the angstrom region," *Appl. Opt.* **25**, 4168–4172 (1986).
5. J. H. Bruning, D. R. Herriott, J. E. Gallagher, D. P. Rosenfeld, A. D. White, and D. J. Brangaccio, "Digital wavefront measuring interferometer for testing optical surfaces and lenses," *Appl. Opt.* **13**, 2693–2703 (1974).
6. J. C. Wyant, "Use of an ac heterodyne lateral share interferometer with real-time wavefront correction systems," *Appl. Opt.* **14**, 2622–2626 (1975).
7. B. Bhushan, J. C. Wyant, and C. L. Koliopoulous, "Measurement of surface topography of magnetic tapes by Mireau interferometry," *Appl. Opt.* **24**, 1489–1497 (1985).
8. K. Tatsuno and Y. Tsunoda, "Diode laser direct modulation heterodyne interferometer," *Appl. Opt.* **26**, 37–40 (1987).
9. Y. Ishii, J. Chen, and K. Murata, "Digital phase-measuring interferometry with a tunable laser diode," *Opt. Lett.* **12**, 233–235 (1987).
10. P. Hariharan, "Phase-stepping interferometry with laser diodes: effect of changes in laser power with output wavelength," *Appl. Opt.* **28**, 27–28 (1989).
11. O. Sasaki and H. Okazaki, "Sinusoidal phase modulating interferometry for surface profile measurement," *Appl. Opt.* **25**, 3137–3140 (1986).
12. O. Sasaki, K. Takahashi, and T. Suzuki, "Sinusoidal phase modulating laser diode interferometer with a feedback control system to eliminate external disturbance," *Opt. Eng.* **29**, 1511–1515 (1990).
13. O. Sasaki and K. Takahashi, "Sinusoidal phase modulating interferometer using optical fibers for displacement measurement," *Appl. Opt.* **27**, 4139–4142 (1988).
14. O. Sasaki, H. Okazaki, and M. Sakai, "Sinusoidal phase modulating interferometer using the integrating-bucket method," *Appl. Opt.* **26**, 1089–1093 (1987).
15. O. Sasaki, T. Okamura, and T. Nakamura, "Sinusoidal phase modulating Fizeau interferometer," *Appl. Opt.* **29**, 512–515 (1990).
16. T. Suzuki, O. Sasaki, K. Higuchi, and T. Maruyama, "Real time displacement measurement in sinusoidal phase modulating interferometry," *Appl. Opt.* **28**, 5270–5274 (1989).
17. T. Suzuki, O. Sasaki, and T. Maruyama, "Phase locked laser diode interferometry for surface profile measurement," *Appl. Opt.* **28**, 4407–4410 (1989).
18. T. Suzuki, O. Sasaki, K. Higuchi, and T. Maruyama, "Phase locked laser diode interferometer: high speed feedback control system," *Appl. Opt.* **30**, 3622–3626 (1991).

Takamasa Suzuki received the BE degree in electrical engineering from Niigata University in 1982 and the ME degree from Tohoku University in 1984. Since 1987 he has worked on interferometers using laser diodes and applications of phase conjugate optics at Niigata University.

Osami Sasaki received the BE and ME degrees in electrical engineering from Niigata University in 1972 and 1974, respectively, and the Dr. Eng. degree in electrical engineering from Tokyo Institute of Technology in 1981. He is an associate professor of electrical engineering at Niigata University, and since 1974 he has worked in the field of optical measuring systems and optical information processing.

Shuich Takayama received the BE degree in electrical engineering from Niigata University in 1992. He was involved with sinusoidal phase modulating interferometers. Since 1992 he has worked on the development of electrical commodities at Twin Bird Corporation.

Takeo Maruyama received the BE degree in electrical engineering from Niigata University in 1965 and the Dr. Eng. degree in electrical engineering from Nagoya University in 1979. He is a professor of electrical engineering at Niigata University, and since 1965 he has worked in the field of the physics of ionized gasses and optical metrology.